

## Research Article

# MHD Flow and Heat Transfer of Water-Based Nanofluid Passing a Permeable Exponentially Shrinking Sheet with Thermal Radiation

M. G. Murtaza<sup>1</sup> , Jahanara Begum<sup>1</sup>, E. E. Tzirtzilakis<sup>2</sup> , M. Ferdows<sup>3\*</sup>

<sup>1</sup>Department of Mathematics, Comilla University, Cumilla-3506, Bangladesh

<sup>2</sup>Fluid Mechanics and Turbomachinery Laboratory, Department of Mechanical Engineering, University of the Peloponnese, Tripoli, Greece

<sup>3</sup>Research Group of Fluid Flow Modeling and Simulation, Department of Applied Mathematics, University of Dhaka, Dhaka-1000, Bangladesh

E-mail: ferdows@du.ac.bd

**Received:** 15 March 2023; **Revised:** 8 June 2023; **Accepted:** 14 June 2023

**Abstract:** The key objective of the present study is to elaborate the concept of boundary layer flow and heat transfer of magnetohydrodynamics namely Cu-water nanofluid flow towards an exponentially shrinking sheet with aid of mathematical modeling and computation. The present mathematical model is investigated under the influence of thermal radiation and suction. Using exponential form of similarity variables, the system of partial differential equations (PDEs) are converted in to a set of ordinary differential equations (ODEs). The resulting nonlinear ODEs are computationally solved by using a two-point boundary value problem numerical technique, which constitutes with common finite difference method. The influence of physical parameters such as magnetic field parameter, Eckert number, suction parameter, radiation parameter are described in details with the help of graphical demonstration of velocity and temperature distributions, coefficient of skin friction and rate of heat transfer. Computational results reveal that after suspension of nanoparticles into base fluid as water fluid temperature raised significantly compare to that of pure fluid. It is also observed that for rising values of magnetic field parameter, thermal radiation, particles volume fraction fluid temperature distribution significantly improved; whereas opposite phenomena is true for suction parameter and Prandtl number. The rate of heat transfer accelerated with Eckert number, Prandtl number, while coefficient of skin friction boost with thermal radiation parameter. For verifying purposes, a comparison has been shown between present results and the computational results of previous studies and found a very close agreement.

**Keywords:** magnetohydrodynamics, nanofluid, exponentially shrinking sheet, thermal radiation, common finite difference method

**MSC:** 76-XX

## Nomenclature

$\eta$	Similarity variable
$(x, y)$	Cartesian coordinates (m)
$(u, v)$	Velocity components along the $x$ and $y$ direction respectively (m/s)

Copyright ©2023 M. Ferdows, et al.

DOI: <https://doi.org/10.37256/cm.4220232684>

This is an open-access article distributed under a CC BY license

(Creative Commons Attribution 4.0 International License)

<https://creativecommons.org/licenses/by/4.0/>

$T$	Temperature of the fluid in the boundary layer (K)
$T_w$	Variable temperature of the surface (K)
$T_\infty$	Free stream temperature (K)
$T_0$	Constant surface temperature
$u_w(x)$	Shrinking velocity
$v_w(x)$	Variable wall mass transfer velocity
$v_0$	Initial strength suction
$B(x)$	Variable magnetic field
$B_0$	Constant magnetic field
$q_r$	Radiative heat flux
$\sigma^*$	Stefan-Boltzman constant
$k^*$	Mean absorption co-efficient
$\mu_{nf}$	Viscosity of nanofluid (kg/ms)
$\alpha_{nf}$	Thermal diffusivity of nanofluid ( $m^2/s$ )
$\phi$	Volumetric fraction of solid nanoparticles
$(\rho c_p)_{nf}$	Heat capacity of the nanofluid (J/KgK)
$C_p$	Specific heat constant pressure (J/KgK)
$\rho_{nf}$	Density of nanofluid ( $kg/m^3$ )
$\rho_s$	Density of volume fraction ( $kg/m^3$ )
$\rho_f$	Density of base fluid ( $kg/m^3$ )
$k_{nf}$	Thermal conductivity of nanofluid (J/msK)
$k_s$	Thermal conductivity of solid fraction (J/msK)
$k_f$	Thermal conductivity base fluid (J/msK)
$\mu_f$	Viscosity of the base fluid (kg/ms)
$\sigma_{nf}$	Electrical conductivity of the nanofluid (Siemens/m)
$\sigma_s$	Electrical conductivity of solid fraction (Siemens/m)
$\sigma_f$	Electrical conductivity of base fluid (Siemens/m)
$\nu_f$	Kinematic viscosity ( $m^2/s$ )
$Pr$	Prandtl number
$\alpha$	Thermal diffusivity ( $m^2/s$ )
$M$	Magnetic field parameter
$Rd$	Thermal radiation parameter
$Ec$	Eckert number
$S$	Wall suction parameter
$Re$	Reynolds number
$f'$	Dimensional velocity components
$\theta$	Dimensionless temperature
$\psi$	Stream function ( $m^2s^{-1}$ )
$C_f$	Skin friction coefficient
$\tau_w$	Local shear stress
$q_w$	Wall heat transfer
$Nu_x$	Local Nusselt number
$Re_x$	Local Reynolds number
$f''(0)$	Skin friction at the wall

$\theta'(0)$	Wall heat transfer gradient
$S$	Suction parameter

### Superscripts

$()'$	Differentiation with respect to $\eta$
-------	--

### Subscripts

$()_{nf}$	Indicates nanofluid
$()_f$	Represent base fluid
$()_s$	Denote solid fluid particle
$w$	condition at the wall

## 1. Introduction

One of the fascinating areas of physics that studies the behavior of electrically conducting fluids in the presence of a magnetic field is magnetohydrodynamics (MHD). In the fields of industrial and biomedical sciences, it is crucial. Medical applications such as magnetic drug targeting, cancer tumor treatment, magnetic endoscopy, and blood flow during surgery, as well as technical devices like pumps, flow meters, generators, metallurgy and material processing in the chemical industry, industrial power engineering, and nuclear engineering, all depend on MHD flow [1-4]. Animasaun et al. [5] examined the mixed convection nanofluid MHD stagnation-point flow, which was driven by buoyancy, and they noticed that a growing value of inclined angle raised the velocity boundary layer along with the induced magnetic field profiles. The behavior of MHD flow and its heat conduction through a porous channel wall were addressed by Fakour et al. [6]. Makinde et al. [7] and Nadeem et al. [8] investigated the electrically conducting fluid flow past an extended sheet in the presence of buoyancy effects.

Nanofluid technology is a modern multidisciplinary field where thermal engineering, nanoscience, and nanotechnology have formed massively over the last few decades. The development of advanced nanotechnology has led to the discovery of numerous methods for developing open estimations of the thermal and physical characteristics of fluids that conduct poorly, such as water, oil, kerosene, glycerol, and lamps. Importance of nanofluid: Sheikholeslami et al. and Malik et al. [9-12] studied nanofluid flow and displayed its applications. Choi [13] was the first to use the term “nanofluid” by putting nano-sized particles in base fluid and discovering that the base fluid’s improved thermal conductivity was caused by a combination of nanoparticles. The state-of-the-art review of nanofluids is addressed by Das et al. [14], where the authors explain the applications of nanofluids along with the importance of convective heat transfer in nanofluids. Because of this characteristic of nanofluids, they have many important applications, for example, thermal power generation systems, nuclear reactors, storage devices, and gas turbine rotors [15]. Later on, Khan et al. [16], studied the numerical simulation of the nanofluid stretching surface for the boundary layer laminar flow. Alok et al. [17] gave a detailed description of squeezing flow through similar plates with Cu-water nanofluid between two parallel plates. Three dimensional micropolar hybrid nanofluid flow past an exponentially stretching sheet was studied by Manjunatha et al. [18]. The study of MHD stagnation point flow of nanofluid passing a stretching surface with variable thickness analyzed by Ramesh et al. [19] and observed that raising value of Brownian motion increased the temperature and thermal boundary layer thickness. Kumar et al. [20] executed 3D rotating flow towards an exponentially stretching surface with solar energy radiation. Upreti et al. [21] studied the significance of thermal radiation and non-uniform heat source on single-and multi-walled nanotubes H<sub>2</sub>O nanofluid flow in porous medium that passed through a flat plate. Abbas et al. [22] investigated the shape factor of nanoparticles such as Cu, Al<sub>2</sub>O<sub>3</sub>, and TiO<sub>2</sub> on water based nanofluid flow under magnetic field effect through a moving rotating plate. Using Xue’s proposed thermal conductivity model, Upreti et al. [23] examined the three dimensional thermal and flow transfer of H<sub>2</sub>O-CNTs nanofluid for a two-way stretchable surface and they found that in such problems Eckert number plays a key role. Gupta et al. [24] investigated the numerical analysis of the squeezing nanofluid flow between two similar plates.

As elaborated earlier, the flow and heat transfer of a fluid through a stretching or shrinking sheet have a wide range of applications in various industrial and technological processes, including the crystallization of paper, hot rolling, glass fiber drawing, petroleum industry drawing of plastic films, and many others. Crane [25] was the first to discuss the nature of an incompressible fluid while passing through a stretched sheet. Partha et al. [26] analyzed the mixed convection flow and thermal transmission of fluid over an exponentially stretched sheet. As its applicability to diverse engineering challenges grows, researchers are now concentrating on understanding the flow of an incompressible fluid due to a shrinking sheet. Wang [27] was the first to describe the peculiar sort of fluid flow caused by contracting sheets. Saleh et al. [28] examined the stagnation point flow of a steady fluid while passing through a shrinking sheet. For the unsteady case, Fang et al. [29] discussed the mass and heat transfer along the shrinking sheet. The combined impacts of chemical reaction and viscous dissipation on hydromagnetic nanofluid flow subject to stretched or shrinking sheet were analyzed by Kameswaran et al. [30]. MHD mixed convection flow under suction and injection variations due to stretched sheets was discussed in detail by Haroun et al. [31]. The effects of radiation heat transfer on many flows, such as space technology and high-temperature operations, are quite significant. The effects of thermal radiation and viscous dissipation on MHD mixed convection flow over an exponential vertical stretched sheet were analyzed by Sreenivasulu et al. [32].

From the stated aforementioned studies, we observed that the physical effects of radiation parameters, Lorentz forces, suction parameters, etc. have limited research work due to exponential shrinking. Therefore, the novelty of the present analysis is to consider the impact of magnetic field and thermal radiation on water-based nanofluid flow over a two-dimensional exponential sheet. The present mathematical model has fundamental importance. For the non-linearity of the addressed mathematical model, a numerical procedure was used for the governing dimensionless equations: the common finite difference method with central differencing. The physical quantities of skin friction coefficient and rate of heat transfer are also examined and presented graphically for numerous pertinent parameters. Additionally, a comparison with recent published studies is also mentioned in tabular form for the accuracy of computational processes. Hopefully, the current study will be applicable in different fields such as drug delivery, contrast enhancement in magnetic resonance, manufacturing, magnetic separation, and transportation.

## 2. Model description

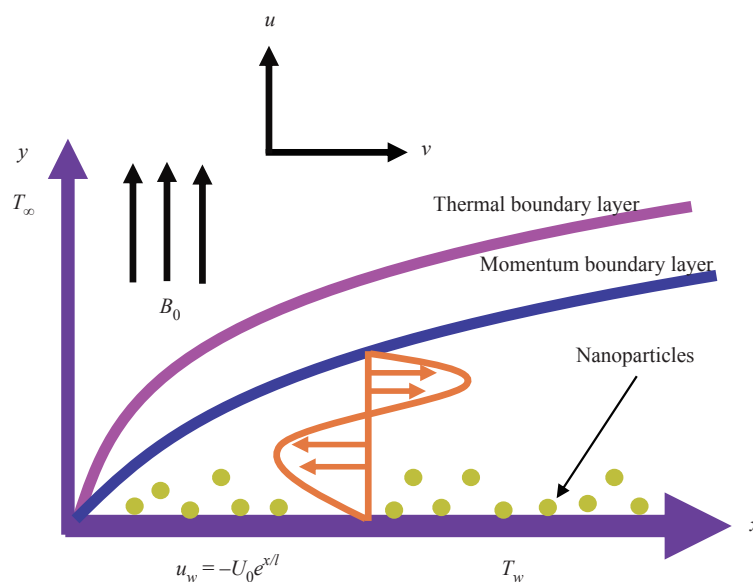


Figure 1. Physical model and co-ordinate system

Consider a steady, two dimensional, laminar, incompressible, and electrically conducting boundary layer flow of Cu-water nanofluid over an exponentially shrinking sheet subject to thermal radiation. Where, the sheet is taken along  $x$ -axis and  $y$ -axis is normal to the sheet. Considered that, velocity of the shrinking sheet is  $u_w = -U_0 e^{x/l}$ , where  $e$  is the exponential parameter and  $U_0$  referred to velocity. A transverse magnetic field  $B(x) = B_0 e^{x/2l}$ , where  $B_0$  is a constant magnetic field which is applied perpendicular to the sheet. However, in flow domain due to the electrical conductivity of blood, a magnetic field is applied and as a result Lorentz force induced in the considered boundary layer.  $T$  is the temperature of the nanofluid, the temperature of the sheet is  $T_w(x) = T_\infty + T_0 e^{x/2l}$  where,  $T_w$  denotes the surface temperature,  $T_\infty$  is free stream temperature and  $T_0$  is the constant temperature. The schematic system of flow is illustrated at Figure 1. From the above assumption, governing continuity, momentum and energy equations for the problem can be written as [33]:

$$\frac{\partial u}{\partial x} + \frac{\partial v}{\partial y} = 0 \quad (1)$$

$$u \frac{\partial u}{\partial x} + v \frac{\partial u}{\partial y} = \frac{\mu_{nf} \partial^2 u}{\rho_{nf} \partial y^2} - \frac{\sigma_{nf}}{\rho_{nf}} B^2 u \quad (2)$$

$$u \frac{\partial T}{\partial x} + v \frac{\partial T}{\partial y} - \frac{\sigma_{nf}}{(\rho c_p)_{nf}} B^2 u^2 = \alpha_{nf} \frac{\partial^2 T}{\partial y^2} - \frac{1}{(\rho c_p)_{nf}} \frac{\partial q_r}{\partial y} \quad (3)$$

The boundary conditions are:

$$\begin{cases} v = v_w(x), u = u_w, T = T_w(x), \text{ as } y = 0 \\ u \rightarrow \infty, T \rightarrow T_\infty, \text{ as } y \rightarrow \infty \end{cases} \quad (4)$$

Here  $u$  and  $v$  are velocity components along  $x$ -axis and  $y$ -axis, respectively. Here  $v_w(x) = v_0 e^{x/2l}$  the variable wall mass transfer velocity,  $v_0$  means initial strength suction, where  $v_0 < 0$  for mass suction and  $v_0 > 0$  for mass injection of the sheet.

According to the study of [33], the radiative heat flux term  $q_r$  can be expressed as:

$$q_r = -\frac{4\sigma^*}{3k^*} \frac{\partial T^4}{\partial y} \quad (5)$$

Where, the symbol  $\sigma^*$  and  $k^*$  means for the Stefan-Boltzman constant and mean absorption co-efficient, respectively. Since the temperature differences of the flow are considered as much as smaller, for that one can expressed the term  $T^4$  as linear function and later on using Taylor series form by neglecting higher order terms we have:

$$T^4 \cong 4T_\infty^3 - 3T_\infty^4 \quad (6)$$

From (2-3),  $\mu_{nf}$  stands for viscosity of nanofluid,  $\alpha_{nf}$  denotes thermal diffusivity of nanofluid and  $\rho_{nf}$  denotes density of nanofluid are presented as [33-35],

$$\rho_{nf} = (1 - \phi)\rho_f + \phi\rho_s; (\rho c_p)_{nf} = (1 - \phi)(\rho c_p)_f + \phi(\rho c_p)_s$$

$$\alpha_{nf} = \frac{k_{nf}}{(\rho c_p)_{nf}}; \frac{k_{nf}}{k_f} = \frac{(k_s + 2k_f) - 2\varphi(k_f - k_s)}{(k_s + 2k_f) + \varphi(k_f - k_s)}; \mu_{nf} = \frac{\mu_f}{(1-\varphi)^{2.5}}$$

$$\frac{\sigma_{nf}}{\sigma_f} = \frac{\sigma_s + 2\sigma_f - 2\varphi(\sigma_f - \sigma_s)}{\sigma_s + 2\sigma_f + \varphi(\sigma_f - \sigma_s)} \quad (7)$$

Here,  $\varphi$  is the volume fraction of solid particles and  $\varphi = 0$  corresponding to a regular fluid.  $(\rho c_p)_{nf}$  denotes the heat capacity of the nanofluid, whereas  $\rho_s$  and  $\rho_f$  are densities related to the nano-particles volume fraction and the base fluid respectively,  $k_{nf}$  denotes thermal conductivity of the nanofluid whereas  $k_s$  and  $k_f$  are the thermal conductivities concerned to solid volume fraction and the base fluid respectively [34]. Here,  $\mu_{nf}$  is the dynamical viscosity of nanofluid; where,  $\mu_f$  is the viscosity of the base fluid,  $\sigma_{nf}$  represents the electrical conductivity of the nanofluid whereas  $\sigma_s$  and  $\sigma_f$  are the electrical conductivity related to solid volume fraction and the base fluid respectively.

The shrinking  $u_w$  is defined by,

$$u_w = -U_0 e^{x/l} \quad (8)$$

### 3. Mathematical analysis

The governing equation (1-3) along with (4) are reduced by following similarity transformation:

$$\eta = y \sqrt{\frac{U_0}{2\nu_f l}} e^{x/2l}; \psi = \sqrt{2\nu_f l U_0} e^{x/2l} f(\eta); \theta(\eta) = \frac{T - T_\infty}{T_w - T_\infty} \quad (9)$$

Where  $\eta$  denotes the similarity variables and  $\nu_f$  is the kinematic viscosity concerned of the base fluid and  $\psi$  indicates stream function.  $\theta(\eta)$  is the dimensionless temperature function and  $f(\eta)$  is the dimensionless function.

The velocity components is obtained when  $\psi$  is defined as:

$$u = \frac{\partial \psi}{\partial y}; v = -\frac{\partial \psi}{\partial x}$$

Substituting equations (5)-(9) into (2-4), the transformed governing equations we have,

$$\frac{f'''}{(1-\varphi)^{2.5} \left\{ (1-\varphi) + \varphi \frac{\rho_s}{\rho_f} \right\}} - \left[ 2Mf'' \left\{ \frac{\sigma_s + 2\sigma_f - 2\varphi(\sigma_f - \sigma_s)}{\sigma_s + 2\sigma_f + \varphi(\sigma_f - \sigma_s)} \right\} \frac{1}{\left\{ (1-\varphi) + \varphi \frac{\rho_s}{\rho_f} \right\}} \right]$$

$$-2(f')^2 + ff'' = 0 \quad (10)$$

$$\frac{k_{nf}/k_f}{Pr \left\{ (1-\phi) + \phi \frac{(\rho c_p)_s}{(\rho c_p)_f} \right\}} \left( 1 + \frac{4}{3} Rd \right) \theta'' + f\theta' - \theta f' + \frac{2MEc(f')^2}{\left\{ (1-\phi) + \phi \frac{(\rho c_p)_s}{(\rho c_p)_f} \right\}} \left\{ \frac{\sigma_s + 2\sigma_f - 2\phi(\sigma_f - \sigma_s)}{\sigma_s + 2\sigma_f + \phi(\sigma_f - \sigma_s)} \right\} = 0 \quad (11)$$

With corresponding boundary conditions are

$$\begin{cases} f(0) = S; f'(0) = -1; \theta(0) = 1 \text{ at } \eta \rightarrow 0 \\ f'(\eta) \rightarrow 0; \theta(\eta) \rightarrow 0 \text{ as } \eta \rightarrow \infty \end{cases} \quad (12)$$

Here,  $Pr = \frac{\nu_f}{\alpha_f}$  is the Prandtl number,  $\alpha = \frac{k_f}{(\rho c_p)_f}$  is the thermal diffusivity,  $\nu_f = \frac{\mu_f}{\rho_f}$  is the kinematic viscosity,  $M = \frac{\sigma_f B_0^2 l}{U_0 \rho_f}$  is the magnetic field parameter,  $Rd = \frac{4\sigma^* T_\infty^3}{k^* k_{nf}}$  is the thermal radiation parameter,  $Ec = \frac{U_0^2 e^{3x/2l}}{(c_p)_f T_0}$  is the Eckert number,  $S = -\frac{v_0}{\sqrt{\nu_f U_0/2l}}$  is the wall suction parameter,  $Re = \frac{\nu_f}{U_0 l e^{x/2l}}$  is the Reynolds number.

Two essential physical quantities of the addressed problem are skin friction Coefficient  $C_f$  and local Nusselt number  $Nu_x$  for the sheet explained as [36],

$$C_f = \frac{\tau_w}{\rho_f u_w^2}$$

$$Nu_x = \frac{1}{k_f (T_w - T_\infty)} \left( q_w - \frac{4\sigma^*}{3k^*} \left( \frac{\partial T^4}{\partial y} \right)_{y=0} \right) \quad (13)$$

Where,  $\tau_w$  is the local shear stress and the convective heat flux  $q_w$  defined by:

$$\tau_w = \mu_{nf} \left( \frac{\partial u}{\partial y} \right)_{y=0}$$

$$q_w = -k_{nf} \left( \frac{\partial T}{\partial y} \right)_{y=0} \quad (14)$$

Substituting equations (5)-(9) into (13-14), finally we have:

$$C_f = \frac{1}{\sqrt{2}} Re^{-1/2} f''(0)$$

$$Nu_x = \frac{-k_{nf}}{k_f} \sqrt{\frac{Re}{2}} \left( 1 + \frac{4}{3} Rd \right) \theta'(0)$$

Where,  $Re = \frac{v_f}{U_0 l e^{x/l}}$  is the Reynolds number.

## 4. Numerical method

Here the numerical procedure that addressed in [37] was discussed in details. This numerical technique is a quite simple, accurate and more precisely efficient in order to solve an extensive class of two-point boundary value similarity problems in fluid mechanics. Since, the momentum equation (10) and energy equation (11) is highly non-linear. So, it is very difficult to solve these equations analytically. That's why we transformed the momentum equation (10) and energy equation (11) into a linear equation. For solving complexity of the addressed problem, numerically we applied a common finite difference technique which based on central differencing. Additionally, a matrix manipulation of tridigonal form is also addressed in technique. For obtained more accuracy of the problem, an iterative procedure is also used in this process. The total numerical technique is stable, accurate and quickly converging. In fluid mechanics, it is an accurate and powerful method for solving highly non-linear problems in case of fluid mechanics as mentioned by [38].

To do that, the momentum equation reduces it to a 2<sup>nd</sup> order linear form by considering:

$$F(x) = f(\eta), F'(x) = f'(\eta), F''(x) = f''(\eta)$$

Now we rewrite the equation (10) as follows,

$$\begin{aligned} & \frac{1}{(1-\varphi)^{2.5} \left\{ (1-\varphi) + \varphi \left( \frac{\rho_s}{\rho_f} \right) \right\}} F''(x) + fF'(x) - 2fF(x) \\ & - \frac{2MF(x)}{\left( (1-\varphi) + \varphi \left( \frac{\rho_s}{\rho_f} \right) \right)} \left\{ \frac{\sigma_s + 2\sigma_f - 2\varphi(\sigma_f - \sigma_s)}{\sigma_s + 2\sigma_f + \varphi(\sigma_f - \sigma_s)} \right\} = 0 \\ \Rightarrow & \frac{F''(x)}{(1-\varphi)^{2.5} \left\{ (1-\varphi) + \varphi \left( \frac{\rho_s}{\rho_f} \right) \right\}} - \left[ 2f + \frac{2M \left\{ \frac{\sigma_s + 2\sigma_f - 2\varphi(\sigma_f - \sigma_s)}{\sigma_s + 2\sigma_f + \varphi(\sigma_f - \sigma_s)} \right\}}{\left\{ (1-\varphi) + \varphi \left( \frac{\rho_s}{\rho_f} \right) \right\}} \right] F(x) \\ & + fF'(x) = 0 \end{aligned}$$

which takes the following form:

$$P(x)F''(x) + Q(x)F'(x) + R(x)F(x) = S(x) \quad (15)$$

Where,

$$P(x) = \frac{1}{(1-\varphi)^{2.5} \left\{ (1-\varphi) + \varphi \left( \frac{\rho_s}{\rho_f} \right) \right\}},$$

$$Q(x) = f,$$

$$R(x) = - \left[ 2f + \frac{2M}{\left\{ (1-\varphi) + \varphi \left( \frac{\rho_s}{\rho_f} \right) \right\}} \left\{ \frac{\sigma_s + 2\sigma_f - 2\varphi(\sigma_f - \sigma_s)}{\sigma_s + 2\sigma_f + \varphi(\sigma_f - \sigma_s)} \right\} \right],$$

$$S(x) = 0$$

In this structure of the equation (15) all the equations of the system can be reduced in the similar process. Therefore the equation (10) is solved by, Applying a common finite difference technique that constitutes with central differencing and matrix manipulation of tridiagonal form.

Before to start the solution procedure, first we have to set initial guesses for  $f(\eta)$ ,  $f'(\eta)$ ,  $\theta(\eta)$  between  $\eta = 0$  and  $\eta = \eta_\infty$  ( $\eta_\infty \rightarrow \infty$ ) which should obviously satisfy the boundary condition (12). For the present problem, we insert the following initial guesses:

$$f(\eta) = S - \frac{\eta}{\eta_\infty}, f'(\eta) = \left( -1 - \frac{\eta}{\eta_\infty} \right) + \delta f''(\eta), \theta(\eta) = \left( 1 - \frac{\eta}{\eta_\infty} \right) + \delta_T \theta'(\eta)$$

The function  $f(\eta)$  is obtained by integrating the curve  $f'(\eta)$ . To forward a new estimation for  $f'(\eta)$  and  $f'_{new}(\eta)$  we have to consider the functions  $f$  is known. Therefore, the updated value of  $f(\eta)$  is obtained by integrating the curve  $f'_{new}(\eta)$ .

Hence, the fresh distributions of  $f'(\eta)$  and  $f(\eta)$  are then imposed for getting new inputs and so on. This solution is continued until the convergence up to a small quantity  $|f''_{new} - f''| \leq \varepsilon$  is obtained.

After obtaining the function  $f(\eta)$ , using the same algorithm energy equation (11) is solved, but without iteration as the equation (10) is linear. The energy equation (11) is

$$\frac{K_{nf}/k_f}{Pr \left\{ (1-\varphi) + \varphi \frac{(\rho c_p)_s}{(\rho c_p)_f} \right\}} \left( 1 + \frac{4}{3} Rd \right) \theta'' + f\theta' - \theta f' = - \frac{2M \cdot EC(f)^2}{\left\{ (1-\varphi) + \varphi \frac{(\rho c_p)_s}{(\rho c_p)_f} \right\}} \left\{ \frac{\sigma_s + 2\sigma_f - 2\varphi(\sigma_f - \sigma_s)}{\sigma_s + 2\sigma_f + \varphi(\sigma_f - \sigma_s)} \right\} \quad (16)$$

By setting  $F(\eta) = \theta(\eta)$  is again a second order linear differential equation of the form,

$$P(x)F''(x) + Q(x)F'(x) + R(x)F(x) = S(x) \quad (17)$$

Where,

$$P(x) = \frac{K_{nf}/k_f}{Pr \left\{ (1-\varphi) + \varphi \frac{(\rho c_p)_s}{(\rho c_p)_f} \right\}} \left( 1 + \frac{4}{3} Rd \right) \Rightarrow P(x) = \frac{(k_s + 2k_f) - 2\varphi(k_f - k_s)}{(k_s + 2k_f) + \varphi(k_f - k_s)} \left( 1 + \frac{4}{3} Rd \right),$$

$$Q(x) = f, R(x) = -f', S(x) = -\frac{1}{\left\{ (1-\varphi) + \varphi \frac{(\rho c_p)_s}{(\rho c_p)_f} \right\}} \left\{ \frac{\sigma_s + 2\sigma_f - 2\varphi(\sigma_f - \sigma_s)}{\sigma_s + 2\sigma_f + \varphi(\sigma_f - \sigma_s)} \right\} 2M.Ec(f')^2$$

We get a new approximation  $\theta_{new}$  for  $\theta$  by considering  $f(\eta)$ ,  $f'(\eta)$  are known. This process is continuing until convergence up to a small quantity  $|\theta'_{new} - \theta'| \leq \varepsilon$  is obtained and finally we obtain  $\theta$ .

In this problem we apply discretization step  $\Delta\eta = 0.01$  and by trial and error we consider the value of  $\eta_\infty = 6$  and convergence criterion  $\varepsilon = 10^{-4}$  defined as  $\varepsilon = \max_{i,N} \left( \left| \frac{f_{old}(i) - f_{new}(i)}{f_{old}(i)} \right| \right)$ .

## 5. Values of thermophysical properties

The values of thermo-physical correlation of water and nanoparticles are given in Table 1.

**Table 1.** Values of  $H_2O$  and  $Cu$  [33, 35]

Thermophysical properties	Water ( $H_2O$ )	Copper ( $Cu$ )
$\rho(\text{kg/m}^3)$	997.1	8,933
$c_p(\text{J/kgK})$	4,179	385
$k(\text{W/mK})$	0.693	400
$\sigma(\text{S/m})$	0.05	$5.96 \times 10^7$
$Pr$	6.2	

## 6. Numerical validation

To check the applicability of the applied code, a comparison has been made with Sumera et al. [33] and Ishak et al. [39] for the Nusselt number  $-\theta'(0)$  for various values of Prandtl number when  $Rd = 0.2$ ,  $M = 0$ ,  $Ec = 0.1$ ,  $S = 3$ . This

obtained results are stated in Table 2 and found an acceptable accuracy. Finally, to obtain the grid suitable for the present mathematical model, a grid independence test is studied here and the obtained result are captured in Table 3. Figure 2 shows the stability analysis for various values of convergence number.

**Table 2.** Comparison of the local Nusselt number  $-\theta'(0)$  for various value  $Pr = 1, 2, 3, 5, 10$  with specific values of  $Rd = 0.2, M = 0, Ec = 0.1, S = 3$

$Pr$	Sumera et al. [33] $-\theta'(0)$	Ishak [39] $-\theta'(0)$	Present results $-\theta'(0)$
1	0.9548106	0.9548	0.958710
2	1.4714540	1.4715	1.475632
3	1.86909	1.8691	1.861887
5	2.5001	2.5001	2.506501
10	3.6603	3.6604	3.663791

**Table 3.** Grid independence test while other parameter values are  $Rd = 0.2, M = 1, Ec = 0.1, S = 3, \varphi = 0.1, Pr = 6.2$

Step size $h = \Delta\eta$	$\eta$	$\theta$	CPU time
0.01	0.2	0.984	0.945
	0.4	0.968	
0.02	0.2	0.986	0.542
	0.4	0.971	
0.04	0.2	0.986	0.507
	0.4	0.971	

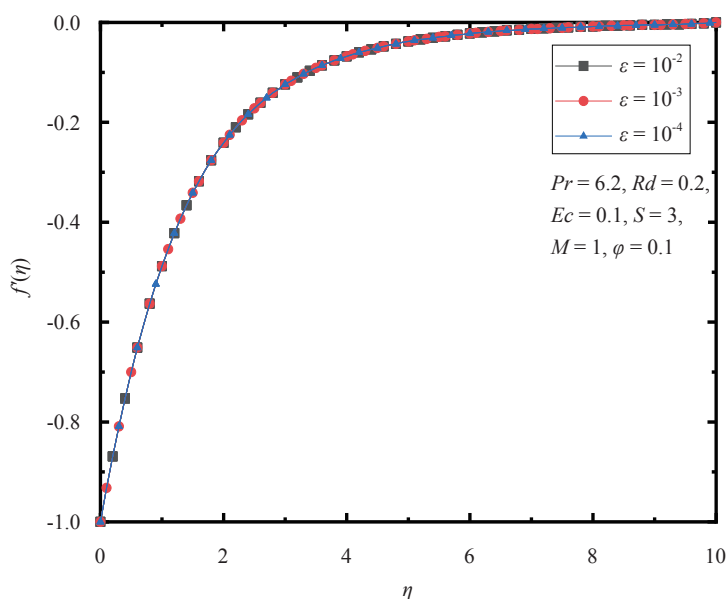


**Figure 2.** Variation of different convergence criteria

## 7. Results and discussion

Since, we have considered the incompressible laminar two-dimensional boundary layer steady state nanofluid flow past an exponentially shrinking surface has been explored numerically. To get an acceptable and authentic numerical results of addressed problem, it is essential to put all realistic values related to parameters. After surviving related to problem, here we used the following values in computational process: Prandtl number  $Pr = 5, 6.2, 7$  as in [40-41], magnetic field parameter  $M = 1, 2, 3$  as in [34], thermal radiation parameter  $Rd = 0.2, 0.4, 0.6$  as in [42], Eckert number  $Ec = 0.5, 1, 1.5, 2, 3$  as in [42-44], wall mass suction parameter  $S = 2.4, 2.6, 2.8, 3$  as in [45].

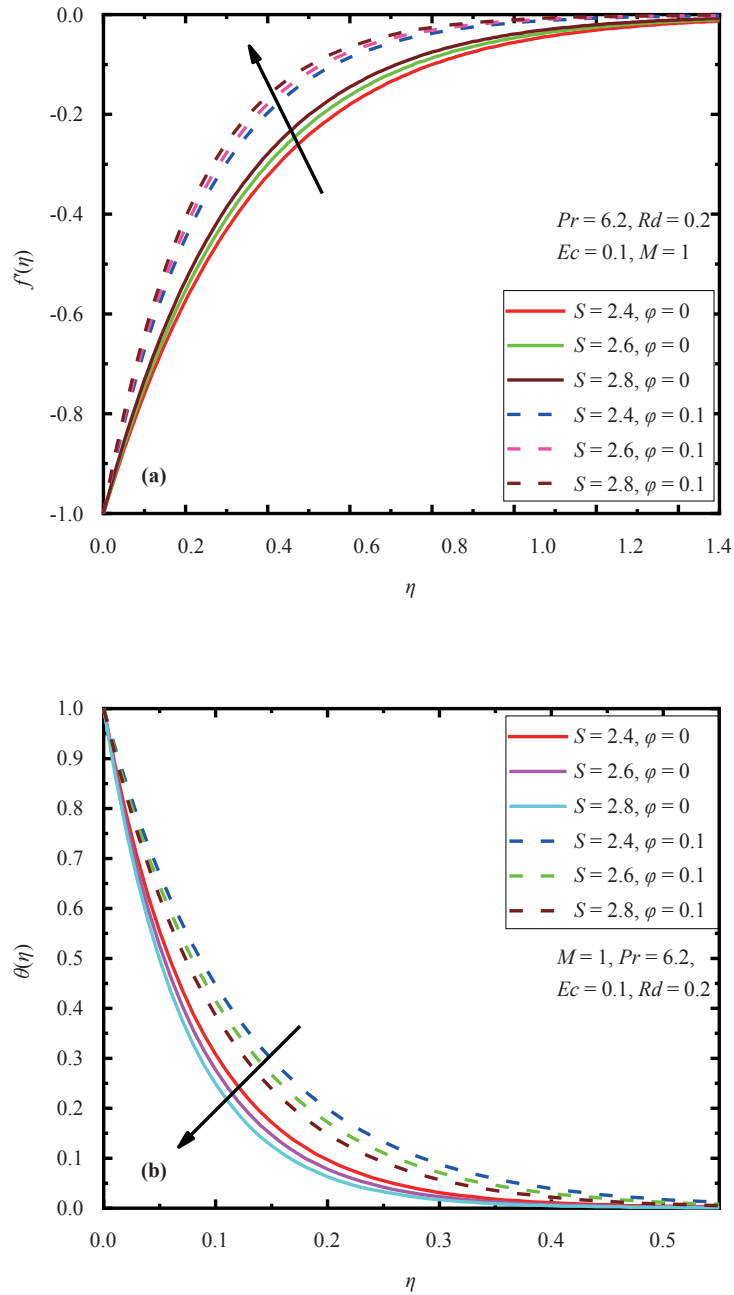
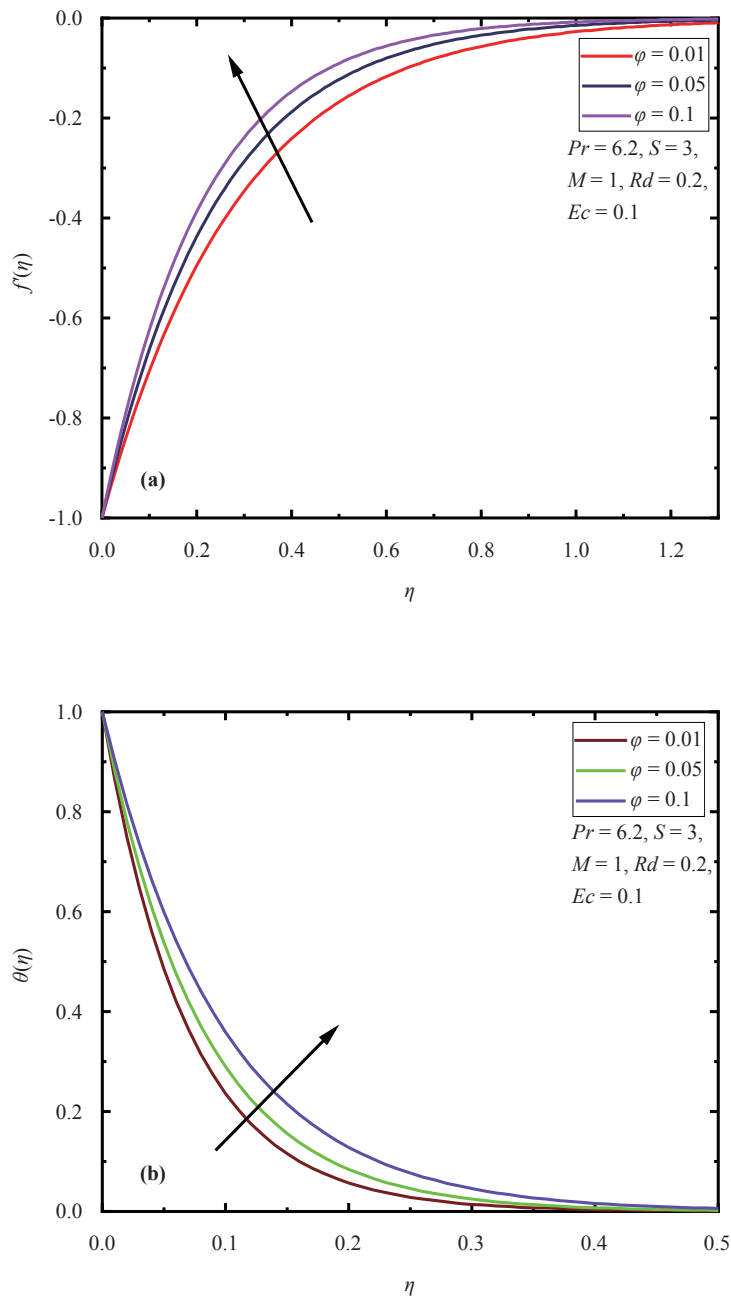


Figure 3. (a) Effect of  $S$  on  $f'(\eta)$ ; (b) Effect of  $S$  on  $\theta(\eta)$

Figures 3(a) and 3(b) show the effects of mass suction parameters on the velocity and temperature profiles. It shows that as suction parameter increased, velocity profile enhanced but temperature profile decline. This is due to the fact that, the fluid in near to the wall is sucked in presence of suction. As a result momentum boundary layer thickness is reduced and consequently distribution of velocity is increased. While fluid temperature is appreciably increased when nanoparticles are mixed with based fluid compare to that of conventional fluid.



**Figure 4.** (a) Effect of  $\varphi$  on  $f'(\eta)$ ; (b) Effect of  $\varphi$  on  $\theta(\eta)$

Figures 4(a) and 4(b) elucidates the variations of solid volume fraction of nanoparticles on  $f'(\eta)$  and  $\theta(\eta)$ , respectively. Both velocity and temperature profiles are accelerate with rising values of volume fraction. The fact is

that the influence of the level of nanofluid viscosity and nanofluid density. Also by mixing nanoparticles into base fluid, thermal conductivity of base fluid is also increased compared to that of regular fluid. As a results thermal boundary layer increased and heat of the fluid is also accelerate.

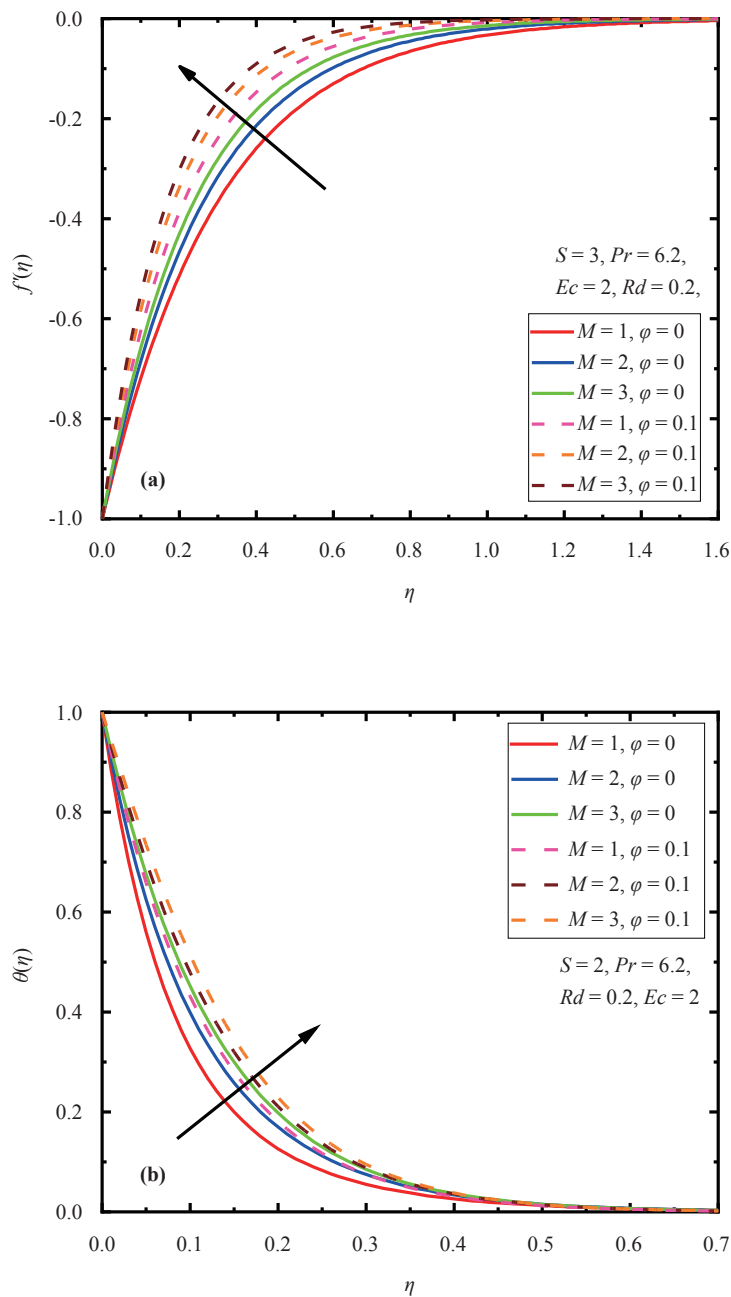


Figure 5. (a) Effect of  $M$  on  $f'(\eta)$ ; (b) Effect of  $M$  on  $\theta(\eta)$

Figure 5(a) and 5(b) portrays the influence magnetic field parameter on  $f'(\eta)$  and  $\theta(\eta)$ , respectively. Both velocity and temperature are reduced due to the incrementing values of  $M$ . The reason behind that when we applied a magnetic field in the flow domain which acts opposite directions of fluid flows, a resistance force induced in the boundary layer. This resistive force are well known as Lorentz force. As a result fluid temperature is accelerate and this increment is

significant in Cu-water case compare to pure fluid case.

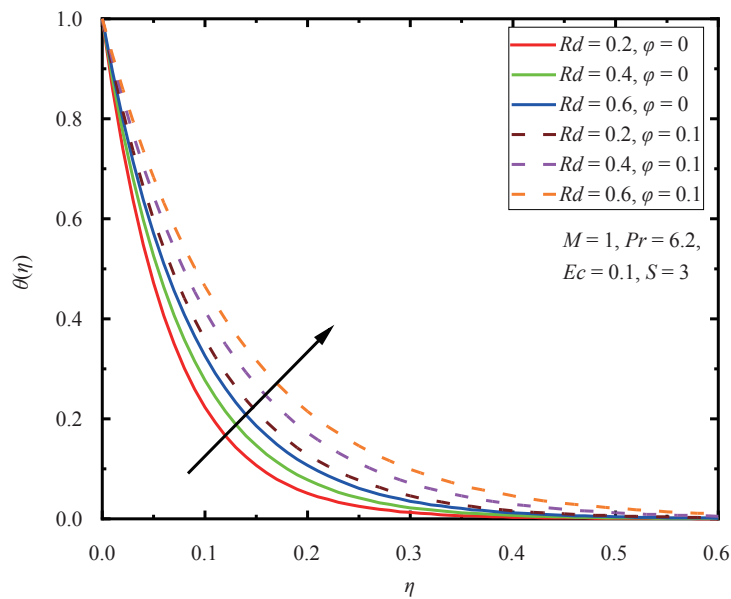


Figure 6. Effect of  $Rd$  on  $\theta(\eta)$

The variations of thermal radiation parameter on temperature profile is displayed in Figure 6. It is observed that  $\theta(\eta)$  profile is increased as radiation parameter enhanced. Because we know that fluids energy is mainly transformed through electromagnetic energy which ultimately increased the fluids internal kinetic development and collisions between the considered fluid molecules. This can be described with radiation parameter, since radiation parameter is representing the thermal dissipation in medium of electromagnetic radiation charge.

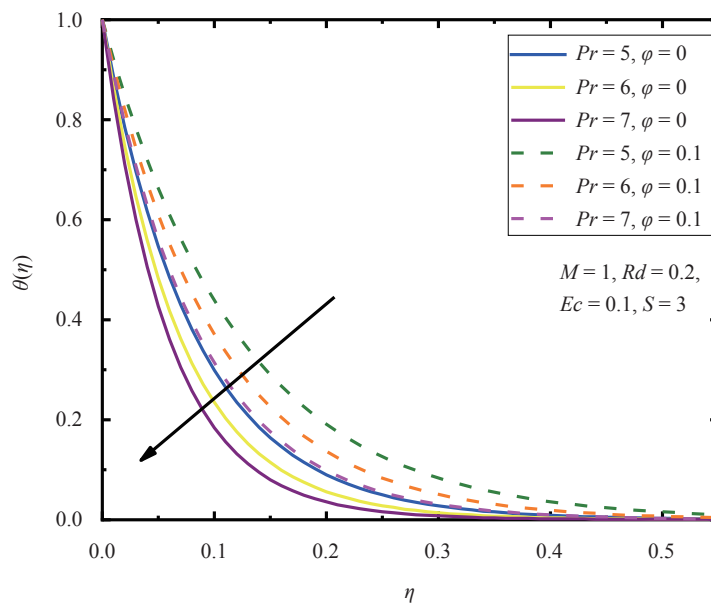


Figure 7. Effect of  $Pr$  on  $\theta(\eta)$

Figure 7 reveals the impact of Prandtl number on heat profile. From the graph, it can be observed that the temperature distribution enhanced due to the accelerate in the Prandtl number. This phenomena is more important for physical applications. As we know that ratio of kinematic viscosity to thermal diffusivity is Prandtl number. Therefore higher values of Prandtl number reduces the thermal diffusivity and its effect is clearly observed in Figure 6.

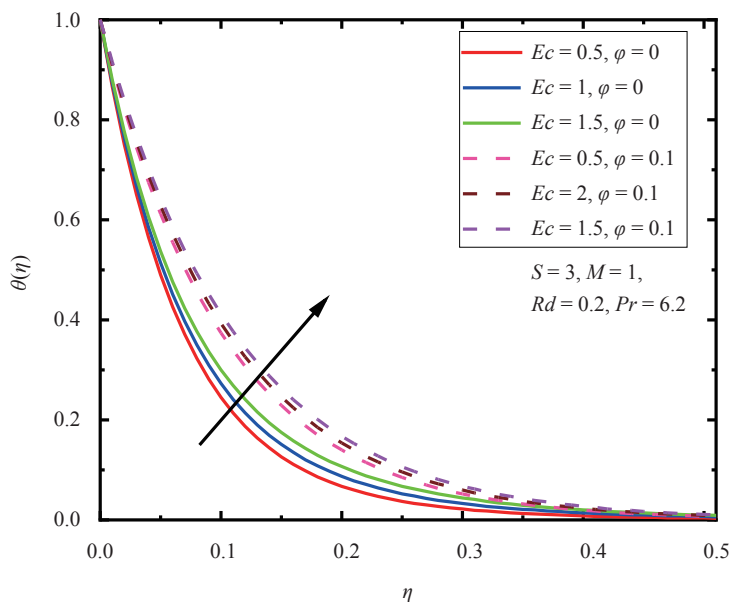
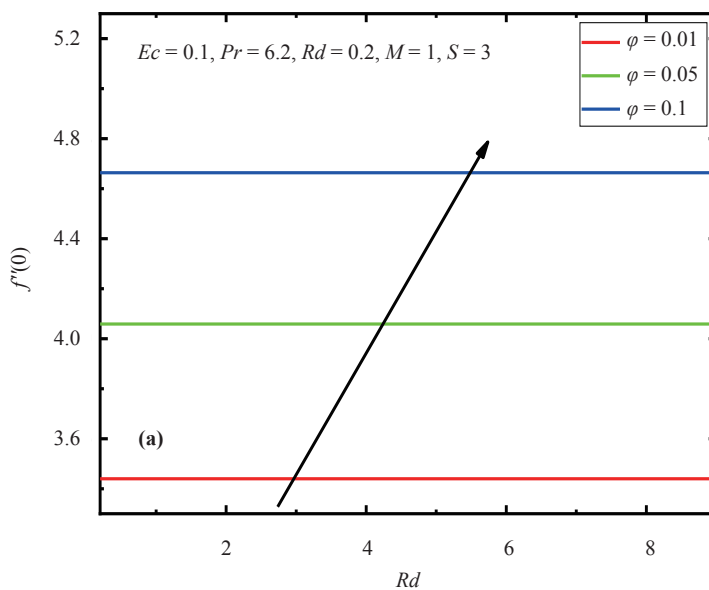
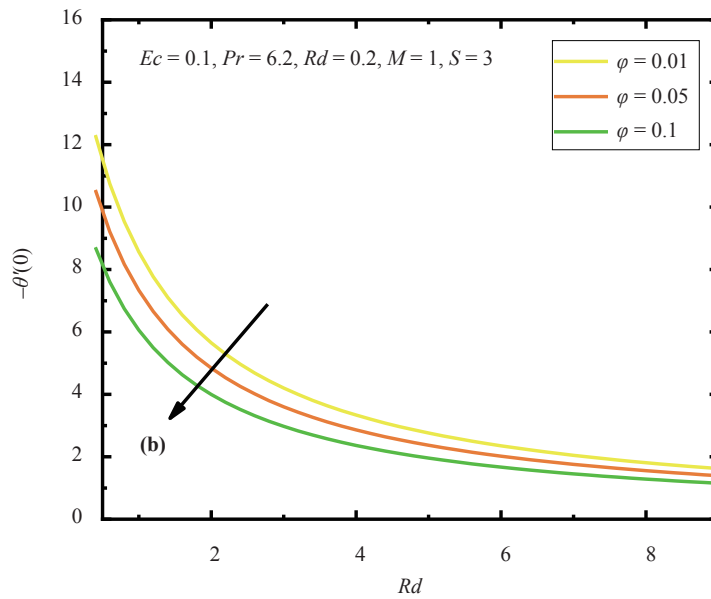


Figure 8. Effect of  $Ec$  on  $\theta(\eta)$

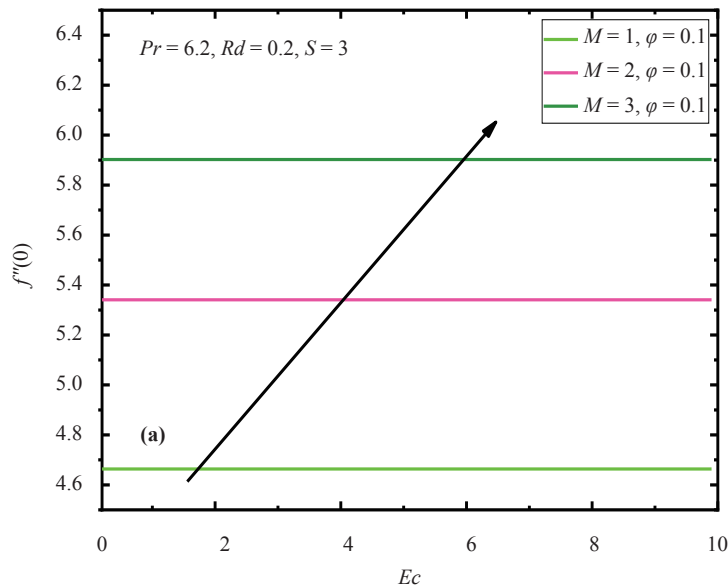
Figure 8 examine the effects of the Eckert number on the heat profile. Figure indicates that with rising values of Eckert number fluid heat from the surface is quickly spread as what expected. Because, the transformation of fluid kinetic energy into the fluid internal energy is caused due to Eckert number and this work is completed against the viscous fluid stresses.





**Figure 9.** (a) Skin friction coefficient  $-f''(0)$  with  $Rd$  for different values of  $\varphi$ ; (b) Local Nusselt number  $\theta'(0)$  with  $Rd$  for different values of  $\varphi$

Figure 9(a) to 11(b), demonstrates the variations of skin friction co-efficient and the rate of heat transfer of Cu-water and Pure water for various values of particles volume fraction, magnetic field parameter, suction parameter against radiation parameter, Eckert number and magnetic field parameter, respectively. From the figures, it is observed that skin friction coefficient is enhanced for the  $\varphi$  and  $M$ ; while reverse act is found in Nusselt number case. Both  $f''(0)$  and  $-\theta'(0)$  are increased for suction parameter cases.



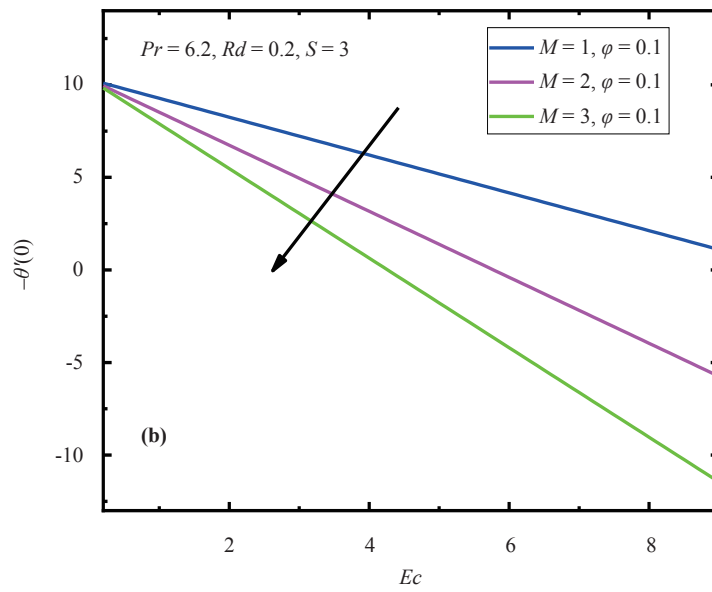
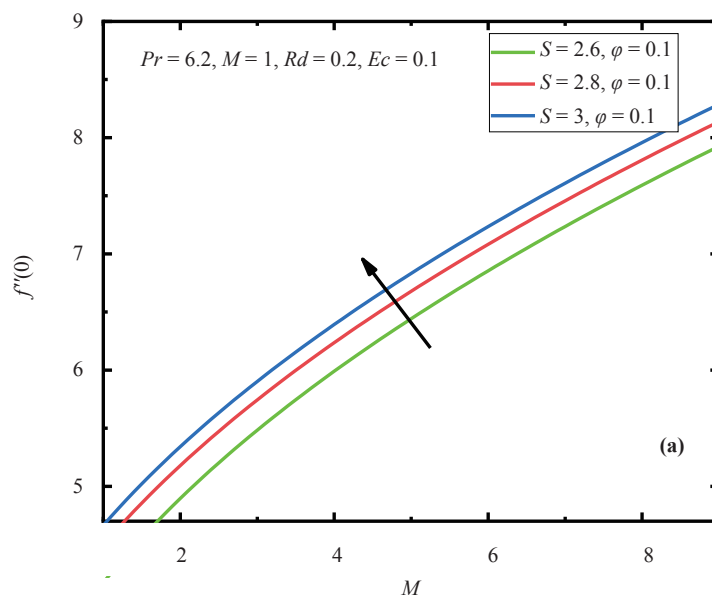


Figure 10. (a) Skin friction coefficient  $-f''(0)$  with  $Ec$  for different values of  $M$ ; (b) Local Nusselt number  $\theta'(0)$  with  $Ec$  for different values of  $M$



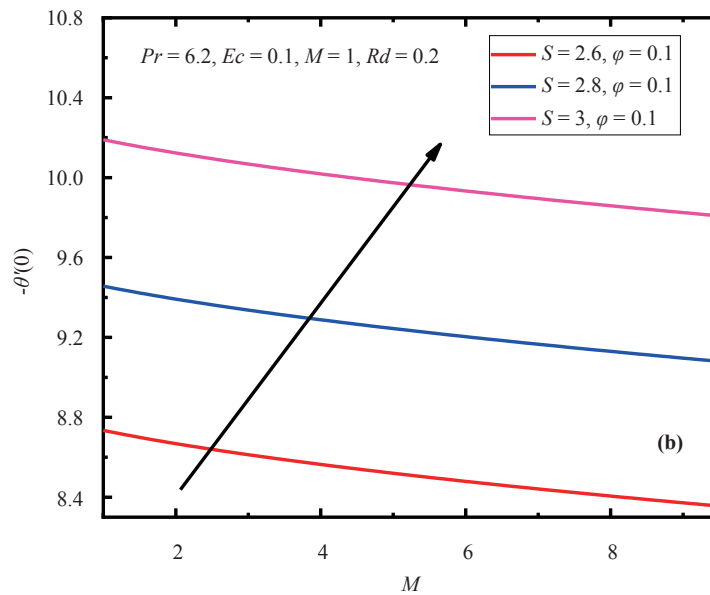


Figure 11. (a) Skin friction coefficient  $-f''(0)$  with  $M$  for different values of  $S$ ; (b) Local Nusselt number  $\theta'(0)$  with  $M$  for different values of  $S$

## 8. Conclusions

In this paper, the influence of suction and thermal radiation on the MHD flow and heat transfer of a water-based Cu-water incompressible nanofluid flow over an exponentially shrinking sheet is analyzed. The numerical results are shown graphically in order to investigate the impacts of physical aspects on velocity and temperature distributions. Some of the findings from the present investigations are:

- An increase in the particle volume fraction, magnetic field parameter, and both velocity and temperature distributions on both occasions, Cu-water nanofluid performance in terms of velocity and temperature is significantly higher than that of pure water flow.
- Fluid velocity increased, but temperature distribution reduced in the presence of the suction parameter.
- Temperature distributions are boosted up with accelerating values of the radiation parameter, Eckert number, while decreasing for Prandtl number.
- The influence of the suction parameter decreases both the skin friction coefficient and the rate of heat transfer.
- An increment in the values of the magnetic field parameter and radiation parameter reduces the coefficient of skin friction but accelerates the rate of heat transfer.

## Conflict of interest

The authors declare no competing financial interest.

## References

- [1] Hatami M, Hosseinzadeh K, Domairry G, Behnamfer M. Numerical study of MHD two-phase Couette flow analysis for fluid-particle suspension between moving parallel plates. *Journal of the Taiwan Institute of Chemical Engineers*. 2014; 45(5): 2238-2245.
- [2] Sheikholeslami M, Ganji D, Ashorynejad HR. Analytical investigation of Jeffery-Hamel flow with high magnetic field and nanoparticle by Adomian decomposition method. *Applied Mathematics and Mechanics*. 2012; 33(1):

1553-1564.

- [3] Kefayati GR. Simulation of heat transfer and entropy generation of MHD natural convection of non-Newtonian nanofluid in an enclosure. *International Journal of Heat and Mass Transfer*. 2016; 92: 1066-1089.
- [4] Sheikholeslami M, Ganji DD. Numerical approach for magnetic nanofluids flow in a porous cavity using CuO nanoparticles. *Materials & Design*. 2017; 120: 382-393.
- [5] Animasaun IL, Prakash J, Vijayaragavan R, Sandeep N. Stagnation flow of nanofluid embedded with dust particles over an inclined stretching sheet with induced magnetic field and suction. *Journal of Nanofluids*. 2017; 6: 28-37.
- [6] Fakour M, Ganji DD, Abbasi M. Scrutiny of underdeveloped nanofluid MHD flow and heat conduction in a channel with porous walls. *Case Studies in Thermal Engineering*. 2014; 4: 202-214.
- [7] Makinde OD, Khan WA, Khan ZH. Buoyancy effects on MHD stagnation point flow and heat transfer of a nanofluid past a convectively heated stretching/shrinking sheet. *International Journal of Heat and Mass Transfer*. 2013; 62: 526-533.
- [8] Nadeem S, Haq RU, Khan ZH. Numerical study of MHD boundary layer flow of a maxwell fluid past a stretching sheet in the presence of nanoparticles. *Journal of the Taiwan Institute of Chemical Engineers*. 2014; 45(1): 121-126.
- [9] Sheikholeslami M, Shah Z, Tassaddiq A, Shafee A, Khan I. Application of electric field for augmentation of ferrofluid heat transfer in an enclosure including double moving walls. *IEEE Access*. 2019; 7: 21048-21056.
- [10] Sheikholeslami M, Gerdroodbary MB, Moradi R, Shafee A, Zhixiong L. Application of neural network for estimation of heat transfer treatment of Al<sub>2</sub>O<sub>3</sub>-H<sub>2</sub>O nanofluid through a channel. *Computer Methods in Applied Mechanics and Engineering*. 2019; 344: 1-12.
- [11] Sheikholeslami M, Mehryan SAM, Shafee A, Sheremet MA. Variable magnetic forces impact on Magnetizable hybrid nanofluid heat transfer through a circular cavity. *Journal of Molecular Liquids*. 2019; 277: 388-396.
- [12] Sheikholeslami M, Shah Z, Shafi A, Khan I, Tlili I. Uniform magnetic force impact on water based nanofluid thermal behavior in a porous enclosure with ellipse shaped obstacle. *Scientific Reports*. 2019; 9(1196): 1-11.
- [13] Choi S. Enhanced thermal conductivity of nanofluids with nano particles, development and applications of Newtonian flows. *ASME Journal of Heat Transfer*. 1995; 66: 99-105.
- [14] Das SK, Choi SU, Yu W, Pradeep T. *Nanofluids: Science and Technology*. New York: John Wiley & Sons, IncHoboken; 2008.
- [15] Owen JM, Roger RH. Flow and heat transfer in rotating-disc systems. *I-Rotor-stator systems, NASA STI/Recon Technical Report A*. Wiley; 1989.
- [16] Khan W, Pop I. Boundary layer flow of a nanofluid past a stretching sheet. *Academia*. 2010; 53: 2477-2483.
- [17] Pandey AK, Kumar AM. Squeezing unsteady MHD Cu-water nanofluid flow between two parallel plates in porous medium with suction/injection. *Computational and Applied Mathematics Journal*. 2018; 4(2): 31-42.
- [18] Manjunatha S, Kuttan BA, Ramesh GK, Gireesha BJ, Emad HA. 3D flow and heat transfer of micropolar fluid suspended with mixture of nanoparticles (Ag-CuO/H<sub>2</sub>O) driven by an exponentially stretching surface. *Multidiscipline Modeling in Materials and Structures*. 2020; 16(6): 1691-1707.
- [19] Ramesh GK, Prasanna BCK, Gireesha BJ, Gorla RSR. MHD stagnation point flow of nanofluid towards a stretching surface with variable thickness and thermal radiation. *Journal of Nanofluids*. 2015; 4(2): 247-253.
- [20] Kumar KG, Ramesh GK, Shehzad SA, Abbasi FM. Three-dimensional (3D) rotating flow of selenium nanoparticles past an exponentially stretchable surface due to solar energy radiation. *Journal of Nanofluids*. 2019; 8(5): 1034-1040.
- [21] Upreti H, Rawat SK, Kumar M. Radiation and non-uniform heat sink/source effects on 2D MHD flow of CNTs-H<sub>2</sub>O nanofluid over a flat porous plate. *Multidiscipline Modeling in Materials and Structures*. 2019; 16(4): 791-809.
- [22] Abbas W, Magdy MM. Heat and mass transfer analysis of nanofluid flow based on Cu, Al<sub>2</sub>O<sub>3</sub> and TiO<sub>2</sub> over a moving rotating plate and impact of various nanoparticles shapes. *Mathematical Problems in Engineering*. 2020; 2020: 9606382.
- [23] Upreti H, Pandey AK, Kumar M, Makinde OD. Darcy-forchheimer flow of CNTs-H<sub>2</sub>O nanofluid over a porous stretchable surface with Xue model. *International Journal of Modern Physics B*. 2023; 37(2): 2350018.
- [24] Gupta AK, Ray SS. Numerical treatment for investigation of squeezing unsteady nanofluid flow between two parallel plates. *Powder Technology*. 2015; 279: 282-289.
- [25] Crane LJ. Flow past a stretching plate. *Journal of Applied Mathematics and Physics*. 1970; 21: 645-647.
- [26] Partha MK, Murthy PVS, Rajasekhar GP. Effect of viscous dissipation on the mixed convection heat transfer from an exponentially stretching surface. *Heat and Mass Transfer*. 2005; 41: 360-366.
- [27] Miklavcic M, Wang CY. Viscous flow due to a shrinking sheet. *Quarterly of Applied Mathematics*. 2006; 64(2):

283-290.

- [28] Saleh SHM, Arifin NM, Nazar R, Ali FM, Pop I. Mixed convection stagnation flow towards a vertical shrinking sheet. *International Journal of Heat and Mass Transfer*. 2014; 73: 839-848.
- [29] Fang TG, Zhang J, Yao SS. Viscous flow over an unsteady shrinking sheet with mass transfer. *Chinese Physics Letters*. 2009; 26(1): 014703.
- [30] Kameswaran PK, Narayana M, Sibanda P, Murthy PVS. Hydromagnetic nanofluid flow due to a stretching or shrinking sheet with viscous dissipation and chemical reaction effects. *International Journal of Heat and Mass Transfer*. 2012; 55(25-26): 7587-7595.
- [31] Haroun NA, Sibanda P, Mondal S, Motsa SS. On unsteady MHD mixed convection in a nanofluid due to a stretching/shrinking surface with suction/injection using the spectral relaxation method. *Boundary Value Problems*. 2015; 1: 1-17.
- [32] Sreenivasulu P, Reddy NB. Thermo-Diffusion and Diffusion-Thermo effects on MHD boundary layer flow past an exponential stretching sheet with thermal radiation and viscous dissipation. *Advances in Applied Science Research*. 2012; 3(6): 3890-3901.
- [33] Dero S, Rohni AM, Saaban A. The dual solution and stability analysis of nanofluid flow using Tiwari-Das model over a permeable exponentially shrinking surface with partial slip conditions. *Journal of Engineering of Applied sciences*. 2019; 14(13): 4569-4582.
- [34] Sandeep N, Sulochana C, Kumar BR. Unsteady MHD radiative flow and heat transfer of a dusty nanofluid over an exponentially stretching surface. *Engineering Science and Technology, an International Journal*. 2016; 19: 227-240.
- [35] Yan L, Dero S, Khan I, Mari IA, Baleanu D, Nisar DS, et al. Dual solutions and stability analysis of magnetized hybrid nanofluid with joule heating and multiple slip conditions. *Processes*. 2020; 8: 332.
- [36] Adnan NSM, Arifin NM, Bacho M, Ali FM. Stability analysis of MHD flow and heat transfer passing a permeable exponentially shrinking sheet with partial slip and thermal radiation. *CFD Letters*. 2019; 11(12): 34-42.
- [37] Kafoussias NG, Williams EW. An improved approximation technique to obtain numerical solution of a class of two-point boundary value similarity problems in fluid mechanics. *International Journal for Numerical Methods in Fluids*. 1993; 17(2): 145-162.
- [38] Tzirtzilakis EE, Kafoussias NG. Three dimensional magnetic fluid boundary layer flow over a linearly stretching sheet. *Journal of Heat Transfer*. 2010; 132: 1-8.
- [39] Ishak A. MHD boundary layer flow due to an exponentially stretching sheet with radiation effect. *Sains Malaysiana*. 2011; 40(4): 391-395.
- [40] Shah Z, Dawar A, Kumam P, Khan W, Islam S. Impact of nonlinear thermal radiation on MHD nanofluid thin film flow over a horizontally rotating disk. *Applied Sciences*. 2019; 12(4): 1533.
- [41] Mamatha B, Raju MC, Varma SVK. Thermal diffusion effect on MHD mixed convection unsteady flow of a micro polar fluid past a semi-infinite vertical porous plate with radiation and mass transfer. *International Journal of Engineering Research in Africa*. 2015; 13: 21-37.
- [42] Murugesan T, Dinesh MK. Viscous dissipation and Joule heating effects on MHD flow of a Thermo-Solutal stratified nanofluid over an exponentially stretching sheet with radiation and heat generation/absorption. *World Scientific News*. 2019; 23(5): 193-210.
- [43] Mathur P, Mishra S. Free convective magnetohydrodynamic flow over an exponentially stretching sheet with radiation. *Heat Transfer Asian Res*. 2019; 6(7): 1-13.
- [44] Rashid I, Sagheer M, Hussain S. Exact solution of stagnation point flow of MHD nanofluid induced by an exponential stretching sheet with thermal conductivity. *Physica Scripta*. 2020; 95: 1-12.
- [45] Jain S, Choudhary R. Effects of MHD on boundary layer flow in porous medium due to exponentially shrinking sheet with slip. *Procedia Engineering*. 2015; 127: 1203-1210.